Short slip duration in dynamic rupture in the presence of heterogeneous fault properties

AUTHOR(S):

Beroza, Gregory C.; Mikumo, Takeshi

JOURNAL OF GEOPHYSICAL RESEARCH, VOL. 101, NO. B10, PAGES 22,449–22,460, OCTOBER 10, 1996

Short slip duration in dynamic rupture in the presence of heterogeneous fault properties

Gregory C. Beroza

Department of Geophysics, Stanford University, Stanford, California

Takeshi Mikumo

Instituto de Geofisica, Universidad Nacional Autonoma de Mexico, Ciudad Universitaria, Mexico

Abstract. Recent studies of strong motion data consistently show that the risetime (duration of slip at particular locations on the fault) is significantly shorter than the overall rupture duration. The physical explanation for this observation and its implications have become central issues in earthquake source studies. Two classes of mechanisms have been proposed to explain short risetimes. One explanation is that velocity-weakening frictional behavior on the fault surface causes the fault to self-heal. This possibility is suggested by rate-dependent friction observed in laboratory experiments and by some two-dimensional dynamic numerical simulations of earthquake rupture. It has recently been demonstrated, however, that the velocity dependence of friction observed in the laboratory is too weak to cause faults to self-heal. An alternative explanation for short risetimes is that spatially heterogeneous fault strength (e.g., barriers) limit the slip duration. In this paper we investigate this second explanation for short risetimes by constructing a three-dimensional dynamic rupture model for the 1984 Morgan Hill, California earthquake (M_W=6.2) using a kinematic model previously obtained from waveform inversion of strong motion data. We assume velocity-independent friction and a critical stress fracture criterion and derive a dynamic model specified by the spatial distribution of dynamic stress drop and strength excess that reproduces the slip and rupture time of the kinematic model. The slip velocity time functions calculated from this dynamic model are then used in a subsequent inversion to fit the strong motion data. By alternating between dynamic and kinematic modeling, we obtain a dynamic model that provides an acceptable fit to the recorded waveforms. In this dynamic model the risetime is short over most of the fault, which is attributable entirely to the short scale-length slip/stress drop heterogeneity required by the strong motion data. A self-healing mechanism, such as strongly velocity-dependent friction, is not required to explain the short risetimes observed in this earthquake.

Introduction

The duration of slip at a point on the fault is often referred to as the risetime. Studies based on teleseismic observations of moderate to large-sized earthquakes have suggested that the risetime scales linearly with either the average fault slip [*Abe*, 1975] or the fault length [*Geller*, 1976]. A linear relationship has also been suggested between the seismic moment and the cube of the pulse width for large shallow earthquakes [*Furumoto and Nakanishi*, 1983] as well as for local deep events [*Kikuchi and Ishida*, 1993]. These results suggest that the duration of slip scales with the fault dimensions; however, the risetime, in the sense that we use it in this paper, is not measured directly in these studies.

Near-source observations [*Aki*, 1968; *Bouchon*, 1978; *Archuleta*, 1984; *Hartzell and Heaton*, 1986; *Beroza and Spudich*, 1988; *Heaton*, 1990; *Beroza*, 1991; *Wald et al.*, 1991; *Cohee and Beroza*, 1994; *Wald and Heaton*, 1994; *Haddon*, 1995] show that the risetime is significantly shorter than that expected from the overall rupture dimensions. This is somewhat surprising because theoretical models of smooth rupture propagation on equidimensional faults suggest that the risetime should be comparable to the rupture duration [e.g., *Madariaga*, 1976]. Although this discrepancy had been noted earlier [*Bouchon*, 1978; *Beroza and Spudich*, 1988], *Heaton* [1990] drew widespread attention to it by compiling evidence from many earthquakes for which the average risetime derived from near-source modeling was only about 16% of that estimated from a dynamic model with smooth rupture propagating at a constant rupture velocity [*Day*, 1982]. The evidence for short slip duration from near-source modeling studies has also been corroborated by eye-witness accounts of rapid slip during surface faulting during a few earthquakes [*Wallace*, 1984; *Yomogida and Nakata*, 1993]. The explanation for unexpectedly short risetimes during earthquake rupture has become one of the central issues in earthquake source studies because it may have important implications for the physics of the rupture process. Two general classes of mechanisms have been postulated.

One class of explanations attributes the short risetime to the frictional behavior of the fault. *Heaton* [1990] proposed velocity-weakening frictional behavior as a mechanism for causing the

Paper number 96JB02291.
0148-0227/96/96JB-02291$09.00

fault to lock spontaneously while slip decelerates after the rupture front passes. This has a number of interesting consequences including slip at low frictional resistance during high velocity sliding, which could explain the stress-heat flow paradox [*Brune et al.*, 1969], and heterogeneous stress drop due to abrupt locking, which can lead to variations in earthquake size as observed in seismicity catalogs [*Madariaga and Cochard*, 1995]. This locking behavior has been shown to cause slip pulses of short duration in numerical simulations of two-dimensional dynamic rupture incorporating simple rate-dependent friction [*Cochard and Madariaga*, 1994; *Madariaga and Cochard*, 1994]. Velocity-weakening frictional behavior has been observed in laboratory experiments [*Dieterich*, 1979, 1981; *Ruina*, 1983], and the circumstances under which these friction laws can give rise to propagating slip pulses of short slip duration have been examined for a range of constitutive parameters by *Perrin et al.* [1995].

Another class of explanations is based on fault zone heterogeneity. Numerical simulations of three-dimensional rupture [e.g., *Day*, 1982] with a simple slip-weakening law show that for a long, narrow fault of width W, the risetime is approximately $W/2v$, where v is the rupture velocity. The risetime is controlled by the shortest dimension of the slipping fault, in this case the width. In fault models with smaller length scales caused by spatially heterogeneous fault properties [*Das and Aki*, 1977; *Papageorgiou and Aki*, 1983; *Boatwright*, 1988] the risetime should be correspondingly shorter. For example, *Johnson* [1990] has shown that short risetimes naturally occur on unilaterally propagating ruptures because a healing pulse from the unruptured side of the fault follows the rupture front.

In this paper we test the feasibility of this second class of explanations by constructing a 3-D dynamic rupture model of the 1984 Morgan Hill, California, earthquake (M_w=6.2) to investigate the effect of heterogeneous fault properties on the risetime. The Morgan Hill earthquake was found by both *Hartzell and Heaton* [1986] and *Beroza and Spudich* [1988] to have heterogeneous slip and extremely short risetimes in their kinematic models. In this study we find that the strong motion data can be fit using a simple velocity-independent, slip-weakening frictional model and that short risetimes are a natural consequence of the stress drop heterogeneity inferred from the strong motion data for this earthquake. Thus, at least for the 1984 Morgan Hill, California earthquake, the strong motion data do not require a self-healing mechanism such as that proposed by *Heaton* [1990]. Because the Morgan Hill earthquake was an extreme example of short risetimes, we believe this conclusion will generalize to other events.

Dynamic Rupture Modeling

In this paper we develop a dynamic model of the 1984 Morgan Hill, California earthquake that is consistent with the strong motion data. To do this we assume a simple failure law: that the fault will rupture once a critical stress level is attained and that the stress will drop to a sliding frictional value. Because the sliding friction in this case does not depend on the slip velocity, we refer to this as velocity-independent friction.

Our dynamic model of earthquake rupture is specified by the strength excess and the stress drop. The strength excess is defined as the difference between the stress just before failure and the prestress. It is a measure of how close the fault is to failure before the earthquake. The other quantity used in our dynamic rupture model is the dynamic stress drop. The dynamic stress drop is defined as the difference between the prestress and the sliding frictional stress after the rupture has occurred.

In early attempts at dynamic rupture modeling, the results from kinematic waveform inversion were used as data and dynamic rupture models were developed to reproduce the gross features of these kinematic models [*Mikumo et al.*, 1987; *Quin*, 1990]. Recently, a more direct approach has been taken to infer the dynamic rupture process by deriving the spatial distribution of dynamic stress drop and strength excess directly from that of fault slip and rupture time obtained from waveform inversion [*Miyatake*, 1992a,b; *Mikumo and Miyatake*, 1993, 1995]. The method is described in these papers, and the results obtained to date are reviewed by *Mikumo* [1994].

In dynamic rupture models that reproduce the kinematic models derived from waveform modeling, the risetime has been shown to be much shorter than the overall rupture duration and comparable to the short slip durations of the kinematic models [*Miyatake*, 1992a; *Mikumo and Miyatake*, 1995]. It is not clear, however, just how well these dynamic rupture models reproduce the recorded waveforms because, although the total slip and rupture times are reproduced, both the slip duration and the form of the slip rate functions are different from those assumed in the kinematic models. In this study we have calculated theoretical seismograms for the fully dynamic rupture models in order to compare them with strong motion data.

We apply a technique similar to that of *Fukuyama and Mikumo* [1993] in which kinematic waveform inversion and dynamic modeling are performed alternately to obtain a dynamic model that fits the recorded seismograms. This alternating inversion approach is indirect and convergence is almost certainly suboptimal. Ultimately, we would like to perform an inversion directly for the dynamic rupture parameters [*Horikawa and Hirahara*, 1993]; however, such an inversion is not computationally feasible for us because it would require a separate dynamic rupture calculation for each partial derivative. The primary goal of this study is not to determine the optimal dynamic rupture model for the 1984 Morgan Hill earthquake, rather we seek to address the question of whether or not the fault heterogeneity found from strong motion modeling can itself explain short risetimes.

Dynamic Rupture Model Inverted From Kinematic Fault Parameters

Whereas *Fukuyama and Mikumo* [1993] use a dynamic model with homogeneous shear stress, static frictional strength, and sliding frictional stress as a starting model when they applied the alternating inversion, we start with the results of kinematic waveform inversion to construct a dynamic rupture model. This is similar to the modeling approach taken by *Ide and Takeo* [1994]. We estimate the distribution of dynamic stress drop and relative fault strength on the fault from the distribution of fault slip and the rupture times obtained from the kinematic waveform inversion, following the method described by *Miyatake* [1992a] and *Mikumo and Miyatake* [1995]. The first step in this approach is to construct a 3-D dynamic rupture model, incorporating the geometry of the kinematic fault model embedded in a horizontally layered crustal structure [*Mikumo et al.*, 1987]. We calculate the dynamic rupture propagating on the fault by solving the three-dimensional wave equation with a finite difference scheme, a critical stress level rupture criterion, and appropriate boundary conditions.

We next estimate the peak shear stress just before each point on the fault ruptures, as the shear stress in the dynamic model that occurs at the rupture time in the kinematic rupture model. The strength excess is the difference between this peak stress and the assumed initial stress. The strength excess estimated in this way is dependent on the grid size and the time increment used in the numerical calculations but may be regarded as measuring the relative values of the strength excess within our model.

The final step is to evaluate the dynamic stress drop from the kinematic fault slip distribution. Since local static stress drop can be estimated by solving the 3-D equilibrium equations [*Miyatake*, 1992a], we start by estimating the static stress drop and then apply an iterative least squares technique to include the effects of rupture propagation. This technique minimizes the summed squared difference between the kinematic slip and the dynamic slip resulting from the estimated dynamic stress drop distribution. Through this procedure we obtain a dynamic rupture model that is consistent with both the slip and the rupture time distribution of the kinematic model. We use this model to calculate the slip-velocity time functions at each point of the fault, which are needed to calculate theoretical seismograms for the dynamic model.

Quasi-dynamic Waveform Inversion Based on a Dynamic Rupture Model

As the next step in our alternating inversion, we perform a waveform inversion to recover a dynamically consistent kinematic fault model (here we call this a quasi-dynamic model), by incorporating the slip rate functions derived from the dynamic model. In the original kinematic fault modeling for this earthquake, *Beroza and Spudich* [1988] assumed that the source time function was identical everywhere on the fault, consisting of an inverse square root singularity of 0.2-s duration. The slip rate functions in the dynamic model generally have a similar time dependence but with different slip durations (risetimes) that depend on the location on the fault.

We use ray theory Green's functions to solve the forward problem using the isochrone integration technique [*Spudich and Frazer*, 1984]. The inverse problem is solved using the linearized inversion technique of *Beroza and Spudich* [1988], which estimates both slip and rupture time as a function of position on the fault. The forward and inverse methods were both modified to account for the spatially variable slip-time functions of the dynamic model by performing a convolution of each segment of the isochrone integration path with the local slip rate function when solving the forward problem and in calculating the partial derivatives needed to solve the inverse problem.

The 1984 Morgan Hill, California, Earthquake: Previous Results

Several kinematic fault models of the 1984 Morgan Hill, California, earthquake have previously been obtained from waveform inversion of strong motion records [*Hartzell and Heaton*, 1986; *Beroza and Spudich*, 1988]. The slip distribution in both of these models was spatially heterogeneous. *Beroza and Spudich* [1988] found a slip maximum exceeding 180 cm, a deep, moderately high-slip zone, and a wide zone of low slip at shallow depths. Rupture propagation in this model was quite smooth until just over 5 s into the earthquake. At this time the rupture jumped ahead of a small unslipped region, then ruptured the unslipped portion from both directions with a component of rupture propagation back towards the hypocenter. The seismic moment was found to be 2.7×10^{18} N m.

A dynamic rupture model consistent with the heterogeneous slip and rupture time model of *Beroza and Spudich* [1988] was obtained by *Mikumo and Miyatake* [1995]. The distribution of static and dynamic stress drops and strength excess was estimated from the fault slip and a slightly smoothed version of the rupture time model using the techniques described above. *Mikumo and Miyatake* [1995] proposed two possible dynamic rupture models for this earthquake; their model I included a nonnegative stress drop constraint, while their model II did not. The areas of large slip at 10 and at 14-17 km to the southeast of the hypocenter were generated by stress drops of 40 and 140 bars, respectively. Model II showed that negative stress drops down to -15 bars were required to account for the areas of very low slip in some shallow parts of the fault. The strength excess was found to be generally small, of the order of 5 bars, but somewhat larger, 15 bars, in the area of delayed rupture propagation about 16 km southeast of the hypocenter. As noted before the strength excess values are grid-size-dependent, but their relative amplitudes should be diagnostic of real differences in the strength excess. The dynamic slip rate functions calculated from model II showed nearly an inverse square-root time dependence with the risetime shorter than 1 s for most of the fault.

Refined Dynamic Rupture Models and Theoretical Seismograms

Although the previous dynamic rupture model II of *Mikumo and Miyatake* [1995] reproduced the slip and rupture time distribution of the kinematic model of *Beroza and Spudich* [1988] fairly well, there still remained an rms difference in the slip distribution of 11 cm between the dynamic and kinematic rupture models. We improved on it by slightly adjusting the stress drop distribution to create a new dynamic model (Figure 1) that more closely reproduces the details of the kinematic model of *Beroza and Spudich* [1988]. The rms of the slip amplitude difference for the improved model is less than 6 cm. The peak dynamic stress drop in the improved model is about 180 bars in the narrow high-slip zone and the area of negative stress drop extends to somewhat deeper areas than in the model published by *Mikumo and Miyatake* [1995]. The strength excess over most of the fault is less than 15 bars. The slip duration is short, less than 1 s for much of the fault. The theoretical seismograms calculated using the modified version of the isochrone integration program, which incorporates the slip rate functions of the dynamic model are shown in Figure 2. The fit to the strong motion data is not very good, even when the fault-parallel components at stations COY and HVY, which were fit poorly by *Beroza and Spudich* [1988] as well, are discounted.

The next step in improving the model was to perform the inversion for a quasi-dynamic model that uses the dynamic model as a starting model and accounts for spatially variable slip rate functions. In this inversion, both slip and rupture time were allowed to vary, as in the original kinematic modeling [*Beroza and Spudich*, 1988]. The resulting slip and rupture time distributions for this quasi-dynamic model are shown in Figure 3. There are substantial differences between this and the original kinematic model. The spatial distribution of slip is more concentrated and the slip amplitudes in the high-slip zones are larger in this model. Peak slip in the high-slip zone 16 km along strike increases to over 230 cm. Two more slip maxima appear with slip of approximately 150 cm 6 and 9 km along strike at depths of about 9 and 11 km, respectively. In the original kinematic model, slip in these areas was smoother and of lower amplitude (Figure 1). The areas of low slip are also somewhat different but still include large areas of the fault at shallow depths. The slip gradients in this model are stronger resulting in higher peak dynamic stress drops. The region of delayed slip at about 16 km along strike from the hypocenter is still present in

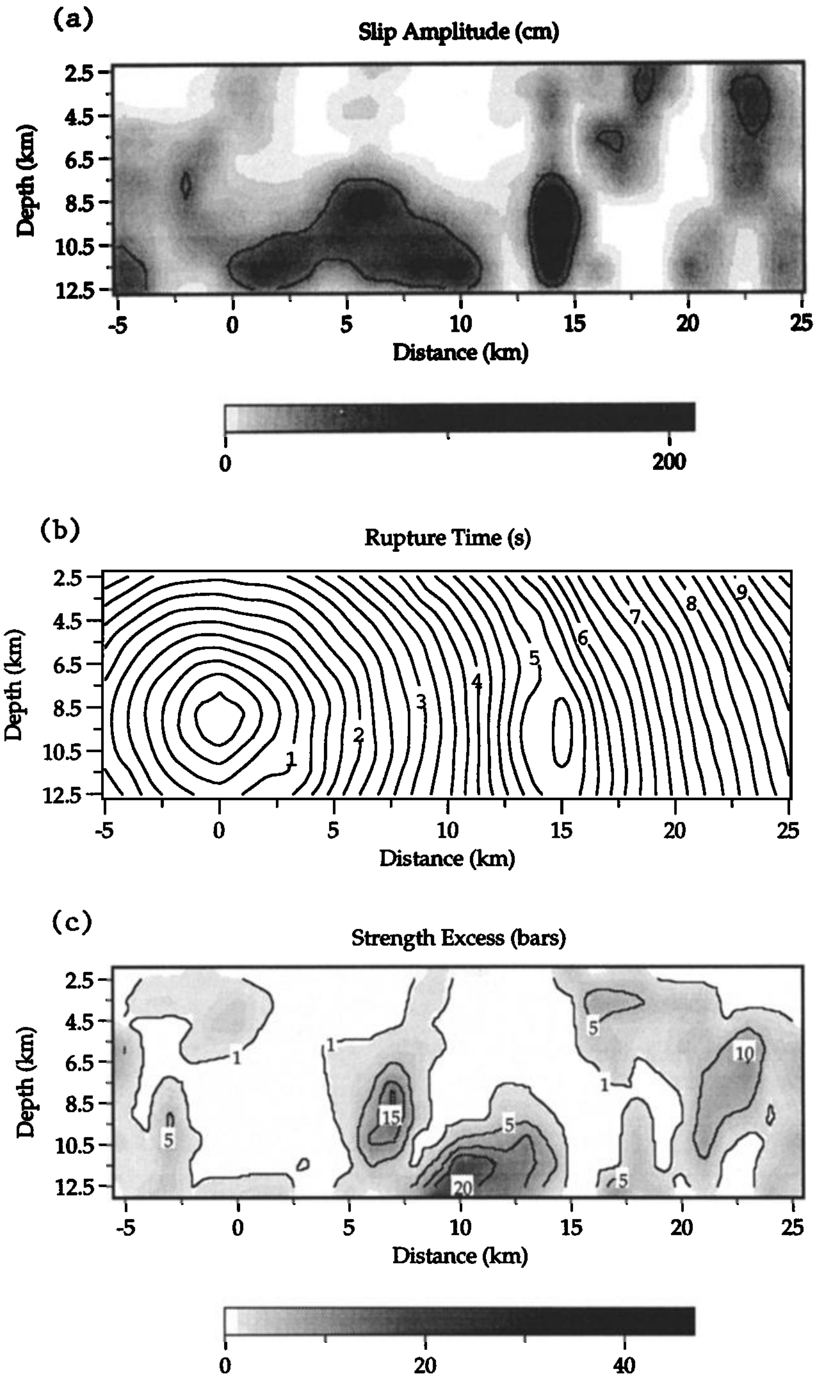

Figure 1. Side view of the initial dynamic rupture model, which accurately reproduces the slip and rupture time distribution of the kinematic model developed by *Beroza and Spudich* [1988]. The hypocenter is at 9 km depth and 0 km along-strike. Positive distances are to the southeast of the hypocenter, and negative distances are to the northwest. For details on the geometry of this sequence, see *Beroza and Spudich* [1988]. (a) Total slip amplitude in cm, the first contour is at 40 centimeters with 40-cm contour intervals; (b) rupture time in s; (c) strength excess in bars, contours are shown for 1, 5, 10, 15, and 20 bars; and (d) dynamic drop stress in bars, contours are -10 bars (dashed) and at intervals of 40 bars starting at 0 bar thereafter. The model assumes a velocity-independent sliding friction and a critical stress fracture criterion.

this model. This is not surprising since this type of behavior is required to fit the strong motion data as discussed by *Beroza and Spudich* [1988].

Since our interest is in finding a dynamic model that is consistent with the strong motion data, we use the quasi-dynamic model shown in Figure 3 as a starting point to derive the fully dynamic final model shown in Figure 4. This dynamic rupture model is derived to reproduce both the slip and the rupture time distribution of the quasi-dynamic model shown in Figure 3. The improved dynamic model has a dynamic stress drop of 220 bars

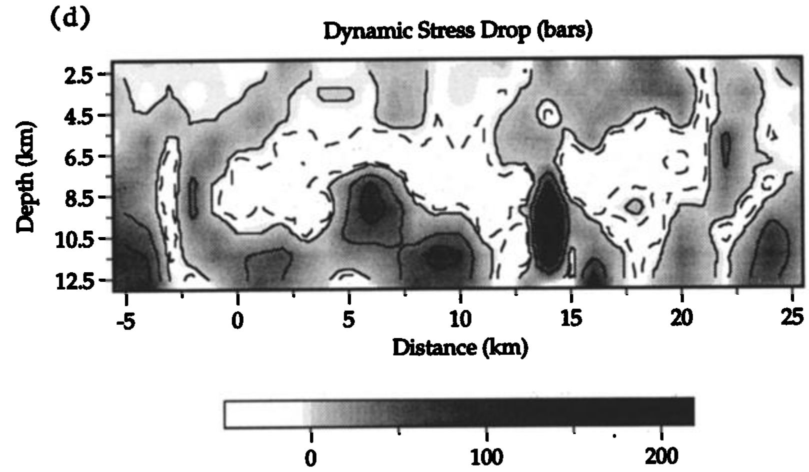

Figure 1. (continued)

in the high-slip zone, which is located about 14 km along strike and a depth of about 9 km. The relatively high-slip regions at 6 and 9 km along strike result from dynamic stress drops of approximately 120 and 110 bars, respectively. Zones of negative stress drop extend over much of the shallow reaches of the fault, especially to the southeast of the hypocenter. There are also areas of negative stress drop at depths that also have high slip and high stress drop. The rms difference of the slip amplitude between the improved dynamic model and the quasi-dynamic model is 2.5 cm. The strength excess tends to increase with depth but also varies strongly along strike. We also note a natural tendency for the rupture to decelerate when it encounters areas of higher strength excess. Figure 5 shows theoretical seismograms calculated for this model. The fit is now substantially improved over the initial dynamic model, particularly on the fault-perpendicular components at stations HVY and ADD, which were also fit well by *Beroza and Spudich* [1988]. The fit is not uniformly improved, however (e.g., the fault-perpendicular component of

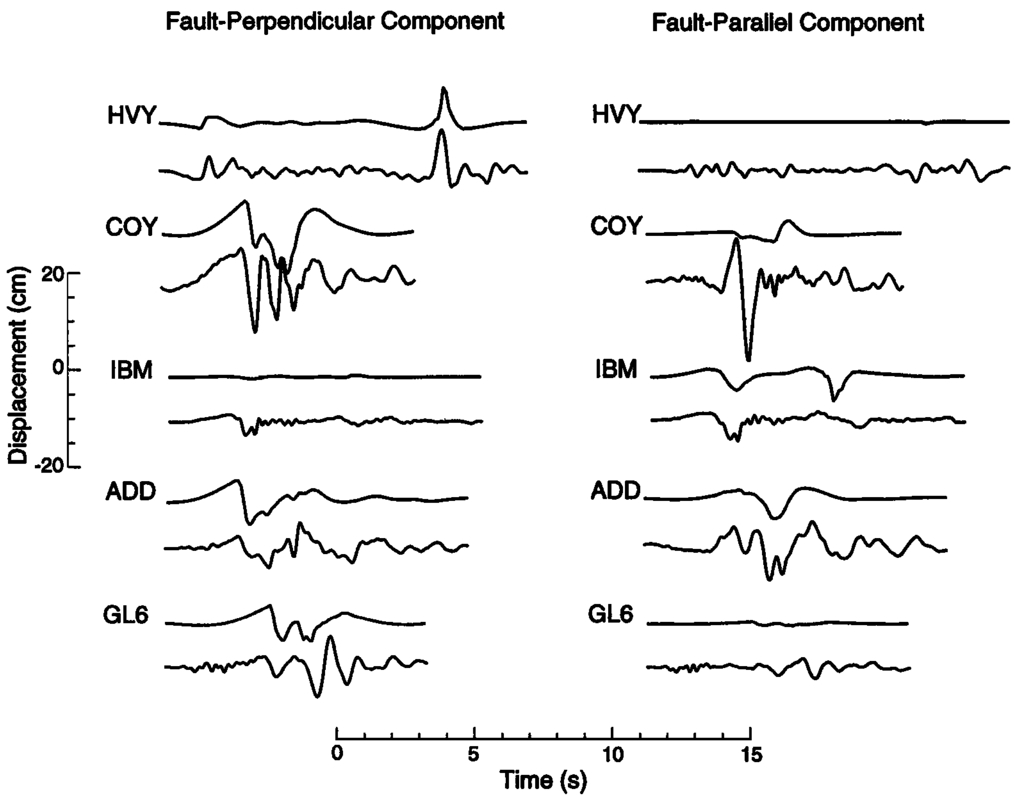

Figure 2. Fit to the data for the initial dynamic rupture model shown in Figure 1 for 5 strong motion stations (see *Beroza and Spudich* [1988] for stations and source-receiver geometry). The data seismograms are shown above theoretical seismograms determined for the dynamic rupture model. The fit to the data is much worse than for the kinematic model. This is because the risetime and time dependence of slip after rupture differ from the kinematic model.

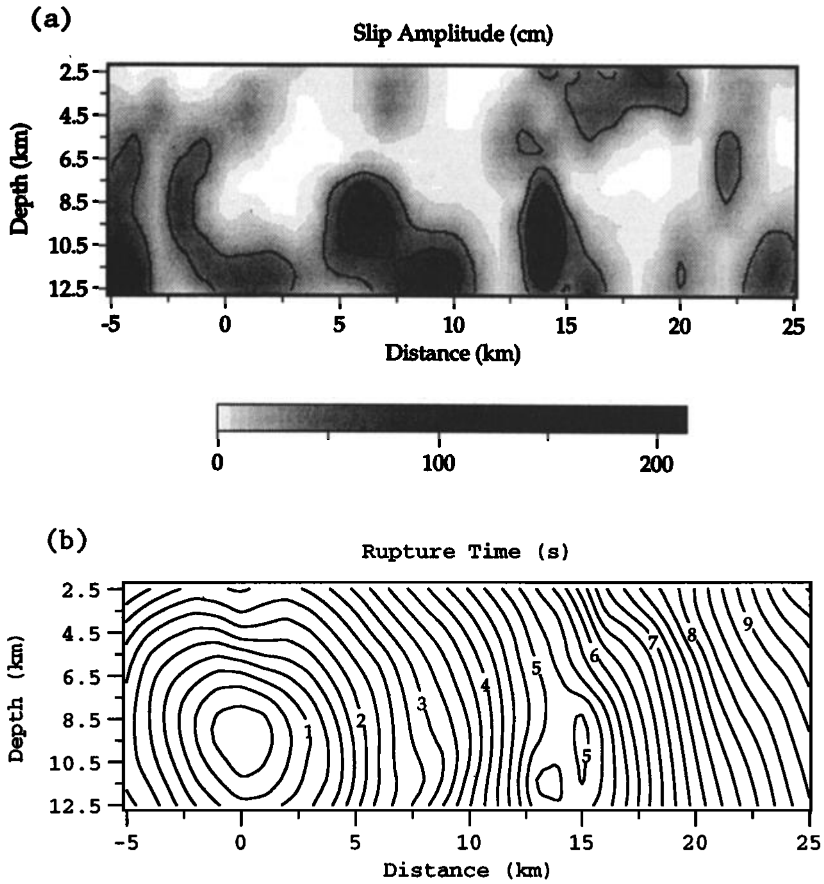

Figure 3. Side view of the quasi-dynamic rupture model, which was derived by assuming the risetimes and time dependence of slip after rupture from the initial dynamic model and performing a linearized inversion for slip and rupture time in order to fit the strong motion data. (a) Total slip amplitude in centimeters, contours start at 40 cm and continue at 40 cm intervals and (b) rupture time in seconds.

station GL6). Further iterations could certainly improve the overall fit somewhat. As before, we are unable to fit the fault-parallel components at HVY and COY. This is attributable to the fact that the theoretical Green's functions for shear waves at these stations from most of the fault are nodal.

The slip duration in our final model, though different than in the previous models, is quite short. Figure 6 shows the risetime, the duration of slip on the fault, for the dynamic model. It is less than 1 s over most of the fault and exceeds 1.5 s in only a few small patches. The duration of slip in the area of highest slip ranges from 0.5 to 1.0 s. Not only is the risetime short, but the slip velocity is strongly concentrated immediately after rupture. Figure 7 shows the slip rate functions for the dynamic model and demonstrates that they have the character of an inverse square root singularity, as expected from fracture mechanics. The slip velocity is concentrated immediately after rupture and is greatly diminished when rupture ceases. The pulse-like, high slip rate portion of the slip velocity has a duration ranging from about 0.2 to 0.5 s.

The short slip duration in this model gives rise to a pulse-like rupture as described by *Heaton* [1990]. This is because as the rupture propagates down the fault, the rupture front, where slip initiates, is never far from part of the fault where slip does not occur and hence where a healing front can be initiated for this velocity-independent frictional model. Figure 8 shows snapshots of the rupture at 0.5-s intervals. In each case, only a small part of the fault is slipping. Moreover, the slip velocity is highest at the rupture front and decays rapidly behind it. Thus the high-slip-velocity part of the rupture front in this model is extremely narrow. Two seconds after the origin time the rupture has organized into a narrow pulse propagating down the fault. The snapshot at 4.25 s shows that the slipping part of the fault is, at times, extremely narrow.

Discussion

We have shown that a dynamic rupture model with heterogeneous stress drop and strength excess is capable of explaining the strong motion records of the 1984 Morgan Hill, California, earthquake. This dynamic model is able to fit the data because the risetime is short. The strength excess was found to be fairly small and smoothly distributed, except near the region of high slip and delayed rupture. On the other hand, the distribution of dynamic stress drop was quite heterogeneous, with negative values on the shallower portions of the fault. Unslipped areas, or areas of negative stress drop, will generate healing fronts that can propagate back across the fault and limit the risetime to a short duration.

Geological or geometrical heterogeneities, such as fault branching or fault bending [*Segall and Pollard*, 1980; *Sibson*,

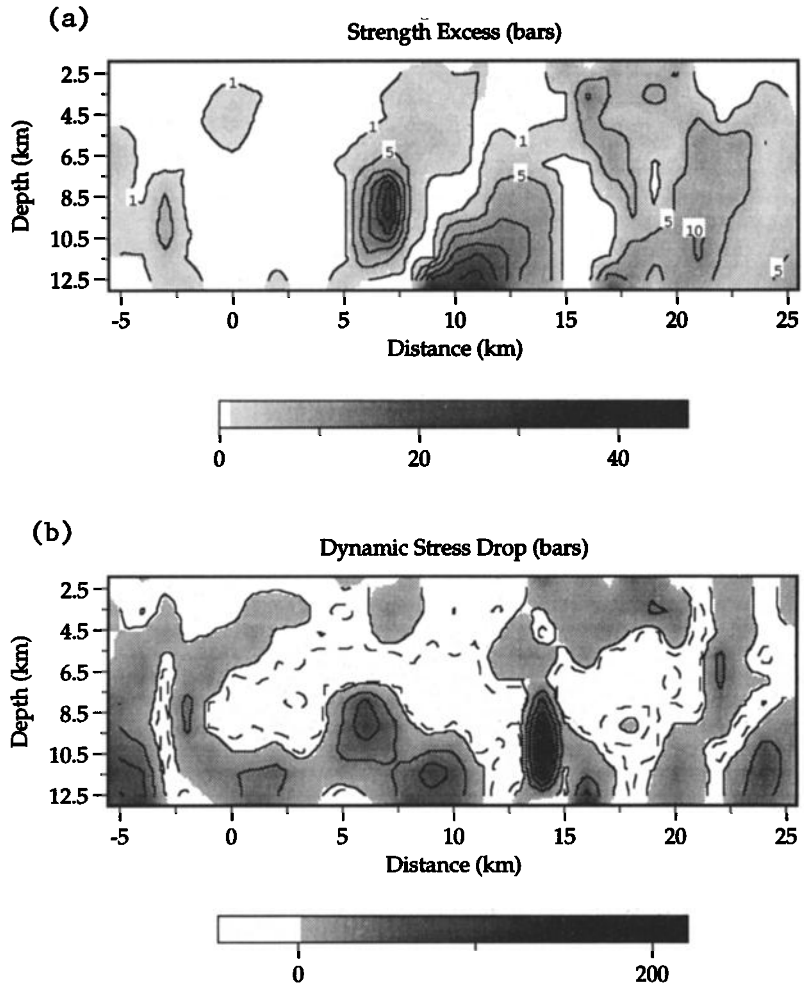

Figure 4. Side view of the improved dynamic rupture model, which reproduces the slip and rupture time distribution of the quasi-dynamic model shown in Figure 3. (a) Strength excess in bars, contours are shown for 1, 5, 10, 15, 20, and 25 bars and (b) dynamic drop stress in bars, contours are -10 bars (dashed) and at intervals of 40 bars starting at 0 bar thereafter. Note that there are substantial areas of negative stress drop, even at seismogenic depths.

1986; *Barka and Kadinsky-Cade*, 1988], nonuniform fault materials [*Michael and Eberhart-Phillips*, 1991], and inhomogeneous pore pressures [*Byerlee*, 1993], are all possible sources of slip and stress drop heterogeneity. This scenario is similar to the barrier model [*Aki*, 1979; *Papageorgiou and Aki*, 1983] in which ruptured areas are interspersed with locked regions of concentrated postseismic shear stress. The stress drop will be negative on and around these regions. Another possible source of negative stress drop is the change from velocity-weakening to velocity-strengthening friction [*Mikumo and Miyatake*, 1995]. The change could occur in shallow sediments or fault gouge [*Marone and Scholz*, 1988] or at mid-crustal depths once temperatures reach 300°-350°C [*Blanpied et al.*, 1991].

Whatever the cause of the observed slip and stress drop heterogeneity, it is required by the strong motion data, and it clearly introduces length scales into the rupture model that are much smaller than the overall dimensions of the fault. These smaller length scales lead to healing pulses being generated in close proximity to the ruptured areas and hence to short risetimes. Thus, in this dynamic model, rupture heterogeneity is the cause of the short risetimes. The possibility that such heterogeneity could cause the slip duration to be short was put forward previously [*Bouchon*, 1978; *Beroza and Spudich*, 1988; *Haddon*; 1995, *Cotton and Campillo*, 1995] but had not been demonstrated by dynamic modeling to be consistent with both velocity-independent sliding friction and the strong motion data.

Heaton [1990] proposed a slip-velocity weakening frictional stress model to account for observed short risetimes. That such a model could, in principle, generate short risetimes was confirmed by *Cochard and Madariaga* [1994]. *Madariaga and Cochard* [1994] showed that rate-dependent friction could make the fault state unstable and generate a healing phase; however, they only observed a short slip pulse in cases where the initial stress field was heterogeneous (*R. Madariaga*, personal communication, 1996). More recently, *Perrin et al.* [1995] showed that pure velocity-weakening friction on smooth, unbounded fault surfaces could not produce solutions for traveling slip pulses without additional dependence on the evolving state of the surface. *Perrin et al.* [1995] also showed that if the rate- and state-dependent friction laws [*Dieterich*, 1979, 1981; *Ruina*, 1983] are assumed, then the ability of rupture to propagate as a self-healing

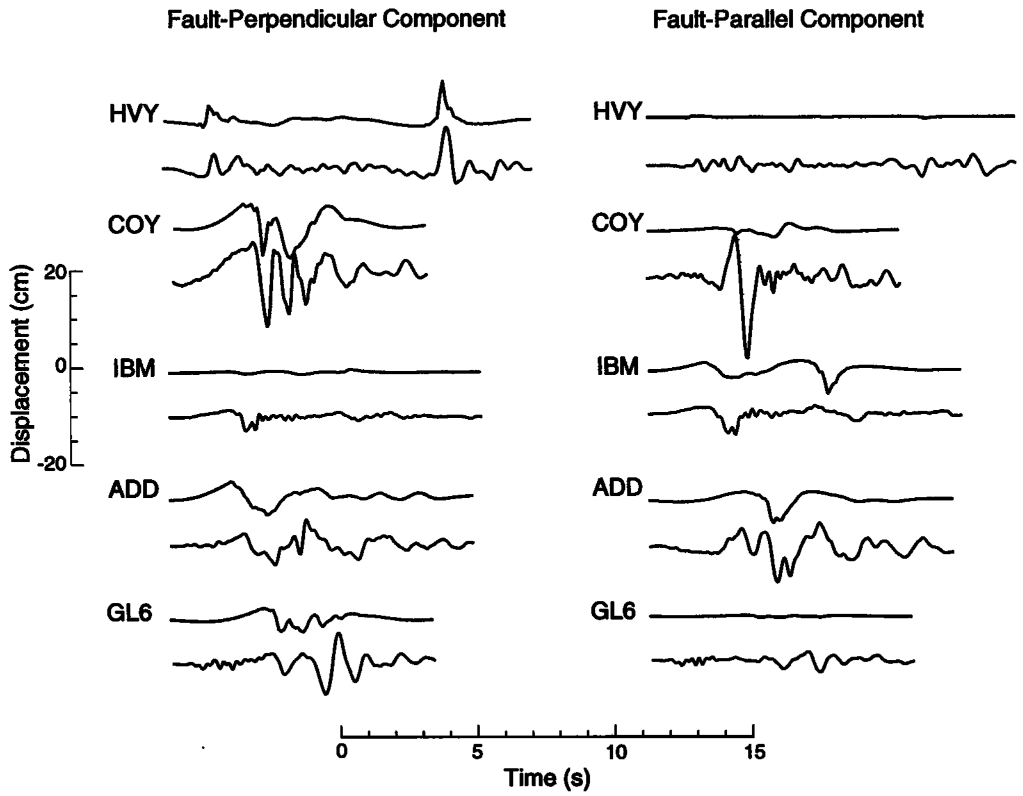

Figure 5. Fit to the strong motion data for the improved dynamic rupture model shown in Figure 4. The fit to the data is greatly improved, especially for stations HVY and ADD.

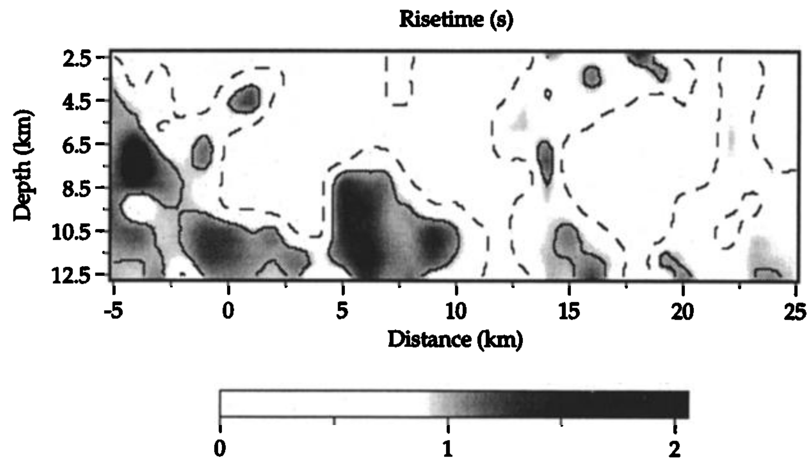

Figure 6. Side view of the risetime for the improved dynamic rupture model (other quantities shown in Figure 4). The risetime is quite short over most of the fault. The half second contour is shown with a dashed line. Areas of risetime > 1 s second are shaded. For most of the fault, the risetime is < 1 s; this is true in the areas of both high slip and low slip.

slip pulse depends on both the state dependence and the characteristic slip rate in the rate dependence. Moreover, they found evidence that even when the self-healing slip pulse did occur, it was not stable. *Perrin et al.* [1995] concluded that if the velocity dependence of frictional properties were extrapolated to velocities of the order of 1 m/s appropriate for earthquake rupture, a self-healing rupture would not occur.

It is not certain, however, what values of characteristic slip rates are appropriate for seismic slip in earthquakes. The rate- and state-variable friction laws referenced above were based on laboratory experiments made at very low sliding velocities ranging from 10^{-9} to 10^{-5} m/s. These sliding velocities are appropriate for the quasi-static nucleation stage of earthquakes and, although some studies have assumed a high-velocity cut off

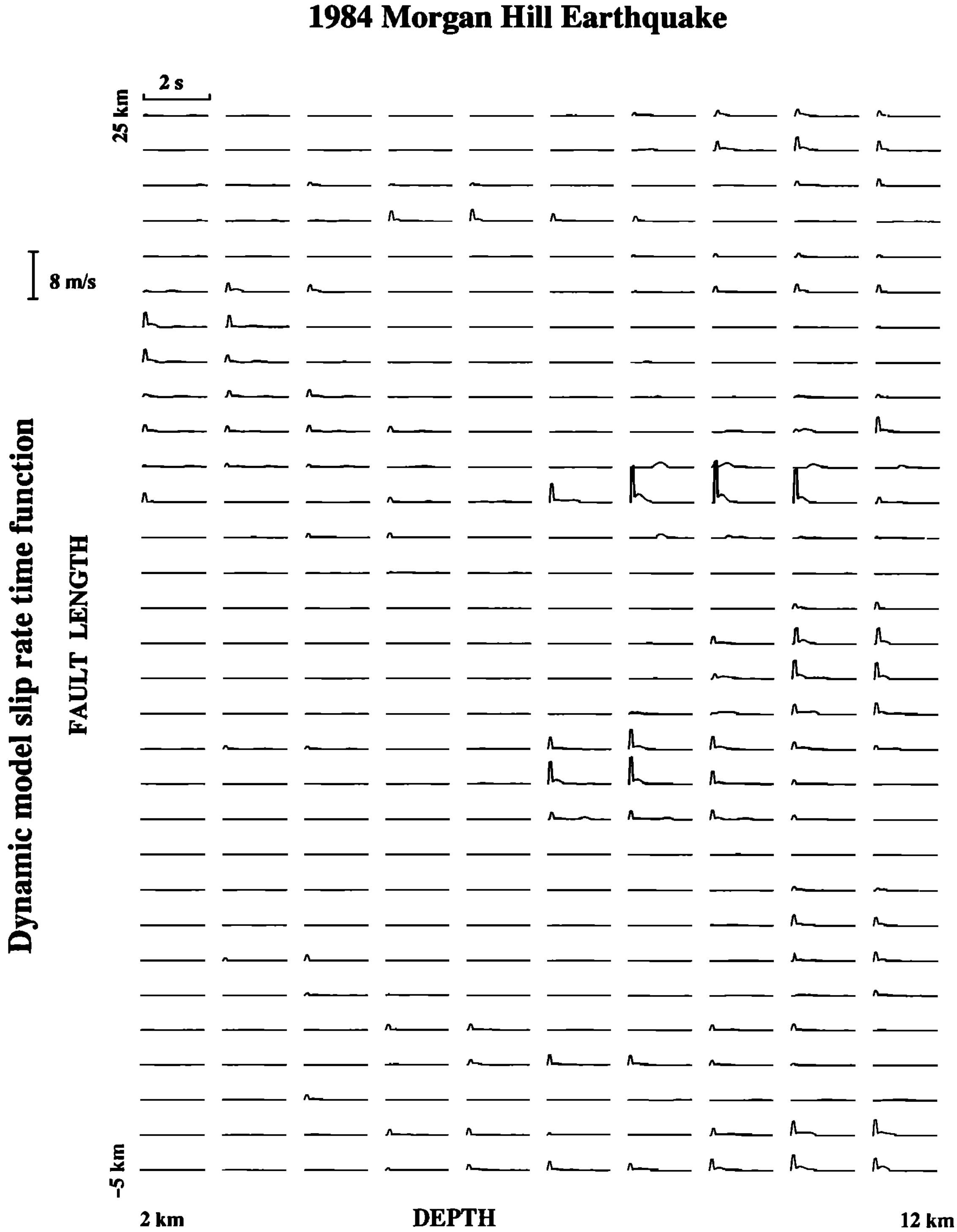

Figure 7. The slip velocity functions are shown for the final dynamic rupture model. The time dependence of slip after rupture shows the inverse square-root of time dependence after slip begins that is expected from fracture mechanics. The duration of the slip velocity is short and is concentrated near the rupture front.

[*Okubo and Dieterich*, 1986; *Okubo*, 1989] or an extension to higher slip rates [*Weeks*, 1993], the validity of extrapolating the low sliding velocity results to the higher sliding velocities of the order 1 m/s that are experienced during earthquake rupture is unclear. Experiments at high slip rates would help to determine the behavior of fault friction at high slip velocities.

Conclusions

The dynamic rupture model presented in this paper demonstrates that short risetimes inferred from modeling strong motion data are consistent with simple dynamic models that incorporate a critical stress level fracture criterion and velocity-

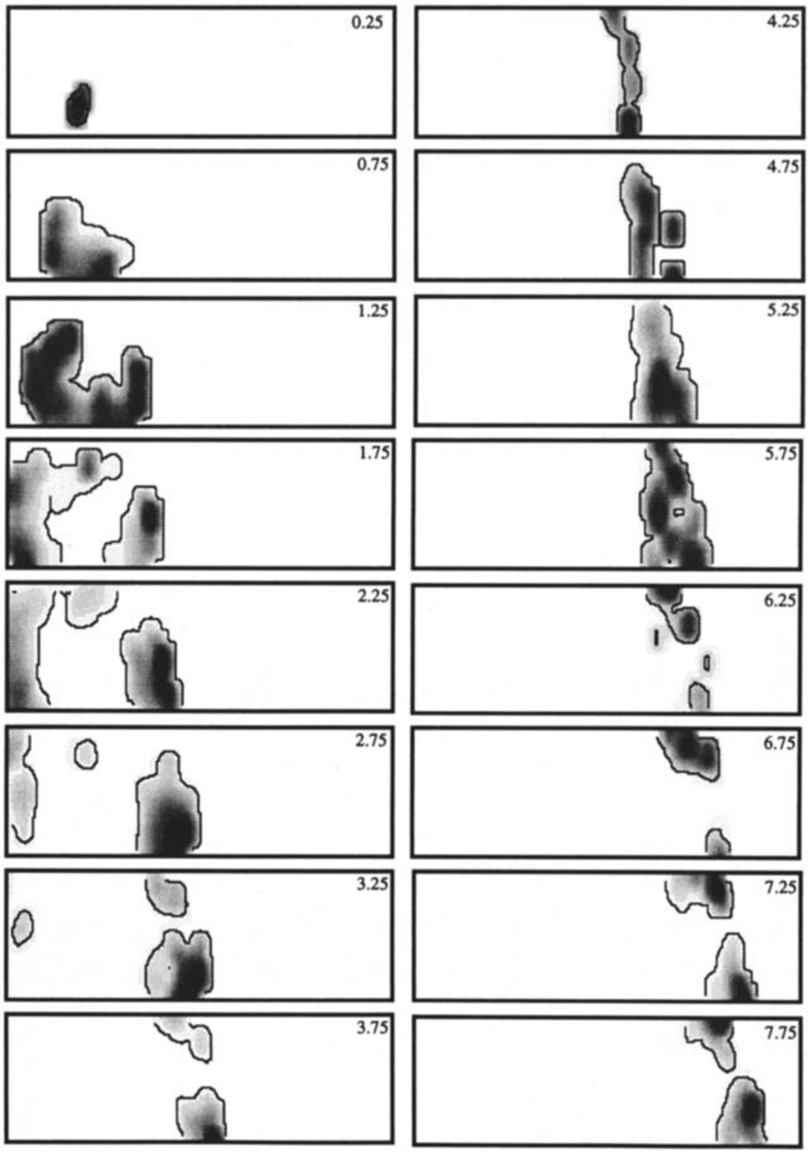

Figure 8. Snapshots of rupture. Panels show snapshots of the rupture at 0.5-s intervals starting 0.25 s into the earthquake. Times are shown in the top right corner of each panel. The darkness of shading in each panel is normalized and proportional to slip velocity. The 1 cm/s contour is shown as a contour. Once 2 s have elapsed, only a small part of the fault is rupturing at a time. By 4 s into the earthquake, slip is constricted to a very small portion of the fault. This pulse-like behavior is attributable to the rupture heterogeneity required by the strong motion data, which causes the fault to heal.

independent sliding friction. We find that short slip durations during the Morgan Hill earthquake are fully attributable and, in fact, are required by the short scale length heterogeneity inferred from strong motion observations. Short risetimes are fully consistent with shear crack models of rupture for which the short scale length of stress/strength heterogeneities include sources of healing pulses that control the slip duration.

We have demonstrated the feasibility of this mechanism for only one earthquake, so it is not necessarily clear that our conclusion will generalize to all earthquakes. We note, however, that dynamic rupture models developed to match the kinematic slip and rupture time distributions estimated for other earthquakes also have risetimes that are as short as those inferred from kinematic modeling [*Quin*, 1990; *Miyatake*, 1992a; *Fukuyama and Mikumo*, 1993; *Ide and Takeo*, 1994].

The Calaveras Fault, on which the 1984 Morgan Hill earthquake occurred, is creeping in places, has a great deal of microearthquake activity [*Oppenheimer et al.*, 1990], and is not necessarily representative of larger, locked faults such as the interplate interface in subduction zones. It is noteworthy, however, that the Morgan Hill earthquake is one of the more extreme examples of short risetimes, so the fact that it is possible to explain the very short risetimes inferred for this earthquake with fault heterogeneity makes it likely that the same explanation can be applied to other earthquakes.

Acknowledgments. We thank Tom Heaton, Jim Rice, and Paul Spudich for helpful discussions. Steve Day, Carl Kisslinger, and Raul Madariaga all provided helpful reviews. Greg Beroza was supported by an NSF Presidential Young Investigator Award.

References

Abe, K., Reliable estimation of the seismic moment of large earthquakes, *J. Phys. Earth, 23*, 349-366, 1975.

Aki, K., Seismic displacements near a fault, *J. Geophys. Res.*, *73*, 5358-5376, 1968.

Aki, K., Characterization of barriers on an earthquake fault, *J. Geophys. Res.*, *84*, 6140-6148, 1979.

Archuleta, R. J., A faulting model for the 1979 Imperial Valley earthquake, *J. Geophys. Res.*, *89*, 4559-4585, 1984.

Barka, A., and K. Kadinsky-Cade, Strike-slip fault geometry in Turkey and its influence on earthquake activity, *Tectonics, 7*, 663-684, 1988.

Beroza, G. C., Near-source modeling of the Loma Prieta earthquake; evidence for heterogeneous slip and implications for earthquake hazard, *Bull. Seismol. Soc. Am.*, *81*, 1603-1621, 1991.

Beroza, G. C., and P. Spudich, Linearized inversion for fault rupture behavior: application to the 1984 Morgan Hill, California, earthquake, *J. Geophys. Res.*, *93*, 6275-6296, 1988.

Blanpied, M. L., D. A. Lockner, and J. D. Byerlee, Fault stability inferred from granite sliding experiments at hydrothermal conditions, *Geophys. Res. Lett.*, *18*, 609-612, 1991.

Boatwright, J., The seismic radiation from composite models of faulting, *Bull. Seismol. Soc. Am.*, *78*, 489-508, 1988.

Bouchon, M., A dynamic source model for the San Fernando earthquake, *Bull. Seismol. Soc. Am.*, *68*, 1555-1576, 1978.

Brune, J. N., T. Henyey, and R. Roy, Heat flow, stress, and rate of slip along the San Andreas fault, California, *J. Geophys. Res.*, *74*, 3821-3827, 1969.

Byerlee, J. D., Model for episodic flow of high-pressure water in fault zones before earthquakes, *Geology, 21*, 303-306, 1993.

Cochard, A., and R. Madariaga, Dynamic faulting under rate-dependent friction, *Pure Appl. Geophys.*, *142*, 419-445, 1994.

Cohee, B. P., and G. C. Beroza, Slip distribution of the 1992 Landers earthquake and its implications for earthquake source mechanics, *Bull. Seismol. Soc. Am.*, *84*, 692-712, 1994.

Cotton, F., and M. Campillo, Frequency domain inversion of strong motions: Application to the 1992 Landers earthquake, *J. Geophys. Res.*, *100*, 3961-3975, 1995.

Das, S., and K. Aki, Fault plane with barriers: A versatile earthquake model, *J. Geophys. Res.*, *82*, 5658-5670, 1977.

Day, S. M., Three-dimensional finite difference simulation of fault dynamics: Rectangular faults with fixed rupture velocity, *Bull. Seismol. Soc. Am.*, *72*, 705-727, 1982.

Dieterich, J. H., Modeling of rock friction, 1, experimental results and constitutive equations, *Pure Appl. Geophys.*, *116*, 790-806, 1979.

Dieterich, J. H., Constitutive properties of faults with simulated gouge, in *Mechanical Behavior of Crustal Rocks*, *Geophys. Monog. Ser.*, vol. 24, pp. 103-120, edited by N. L. Carter, M. Friedman, J. M. Logan, and D. W. Stearns, AGU, Washington, D.C., 1981.

Fukuyama, E., and T. Mikumo, Dynamic rupture analysis: inversion for the source process of the 1990 Izu Oshima, Japan earthquake (*M*6.5), *J. Geophys. Res.*, *98*, 6529-6542, 1993.

Furumoto, M., and I. Nakanishi, Source times and scaling relations of large earthquakes, *J. Geophys. Res.*, *88*, 2191-2198, 1983.

Geller, R. J., Scaling relations for earthquake source parameters and magnitudes, *Bull. Seismol. Soc. Am.*, *66*, 1501-1523, 1976.

Haddon, R. A. W., Modeling of source rupture characteristics for the Saguenay earthquake of November 1988, *Bull. Seismol. Soc. Am.*, *78*, 525-551, 1995.

Hartzell, S. H., and T. H. Heaton, Rupture history of the 1984 Morgan Hill, California, earthquake from the inversion of strong motion records, *Bull. Seismol. Soc. Am.*, *76*, 649-674, 1986.

Heaton, T. H., Evidence for and implications of self-healing pulses of slip in earthquake rupture, *Phys. Earth Planet Inter.*, *64*, 1-20, 1990.

Horikawa, H., and Hirahara, K., Retrieval of dynamic source parameters with waveform inversion, *Eos Trans. AGU*, *74*, 400, 1993.

Ide, S., and M. Takeo, The dynamic rupture process of the 1993 Kushiro-oki, Japan earthquake, *Seismol. Res. Lett.*, *65*, 30, 1994.

Johnson, E., On the initiation of unilateral slip, *Geophys. J. Int.*, *101*, 125-132, 1990.

Kikuchi, M., and M. Ishida, Source retrieval for deep local earthquakes with broadband records, *Bull. Seismol. Soc. Am.*, *83*, 1855-1870, 1993.

Madariaga, R., Dynamics of an expanding circular fault, *Bull. Seismol. Soc. Am.*, *66*, 639-666, 1976.

Madariaga, R., and A. Cochard, Seismic source dynamics, heterogeneity and friction, *Ann. Geofis.*, *37*, 1349-1375, 1994.

Madariaga, R., and A. Cochard, Complex earthquake dynamics for partial stress drop, *Eos Trans. AGU, 76* (46), Fall Meet. Suppl., F404, 1995.

Marone, C. and C. H. Scholz, The depth of seismic faulting and the upper transition from stable to unstable slip regions, *Geophys. Res. Lett.*, *15*, 621-624, 1988.

Michael, A. J., and D. M. Eberhart-Phillips, Relations among fault behavior, subsurface geology, and three-dimensional velocity models, *Science, 253*, 651-654, 1991.

Mikumo, T., Dynamic fault rupture processes of moderate-size earthquakes inferred from the results of waveform inversion, *Ann. Geofis.*, *37*, 1377-1389, 1994.

Mikumo, T., and T. Miyatake, Dynamic rupture processes on a dipping fault, *Geophys. J. Int.*, *112*, 481-496, 1993.

Mikumo, T., and T. Miyatake, Heterogeneous distribution of dynamic stress drop and relative fault strength recovered from the results of waveform inversion: The 1984 Morgan Hill, California, earthquake, *Bull. Seismol. Soc. Am.*, *85*, 178-193, 1995.

Mikumo, T., K. Hirahara, and T. Miyatake, Dynamic fault rupture processes in heterogeneous media, *Tectonophysics*, *144*, 19-36, 1987.

Miyatake, T., Reconstruction of dynamic rupture process of an earthquake with constraints of kinematic parameters, *Geophys. Res. Lett.*, 19, 349-352, 1992a.

Miyatake, T., Dynamic rupture processes of inland earthquakes in Japan: Weak and strong asperities, *Geophys. Res. Lett.*, *19*, 1041-1044, 1992b.

Okubo, P., Dynamic rupture modeling with laboratory-derived constitutive relations, *J. Geophys. Res.*, *94*, 12,321-12,335, 1989.

Okubo, P., and J. H. Dieterich, State variable fault constitutive relations for dynamic slip, in *Earthquake Source Mechanics*, *Geophys. Monog. Ser.*, *vol. 37*, edited by S. Das, J. Boatwright, and C. H. Scholz, pp. 25-35, AGU, Washington, D.C., 1986.

Oppenheimer, D. H., W. H. Bakun, and A. G. Lindh, Slip partitioning of the Calaveras fault, California, and prospects for future earthquakes, *J. Geophys. Res.*, *95*, 8483-8498, 1990.

Papageorgiou, A. S., and K. Aki, A specific barrier model for the quantitative description of inhomogeneous faulting and the prediction of strong ground motion, II, Applications of the model, *Bull. Seismol. Soc. Am.*, *73*, 953-978, 1983.

Perrin, G., J. R. Rice, and G. Zheng, Self-healing slip pulse on a frictional surface, *J. Mech. Phys. Solids*, *43*, 1461-1495, 1995.

Quin, H., Dynamic stress drop and rupture dynamics of the October 15, 1979 Imperial Valley earthquake, *Tectonophysics*, *175*, 93-117, 1990.

Ruina, A. L., Slip instability and state variable friction laws, *J. Geophys. Res.*, 88, 10,359-10,370, 1983.

Segall, P., and D. D. Pollard, Mechanics of discontinuous faults, *J. Geophys. Res.*, *85*, 4337-4350, 1980.

Sibson, R. H., Rupture interaction with fault jogs, in *Earthquake Source Mechanics*, *Geophys. Monog. Ser.*, *vol. 3*, edited by S. Das, J. Boatwright, and C. H. Scholz, pp. 157-167, AGU, Washington, D. C., 1986.

Spudich, P., and L. N. Frazer, Use of ray theory to calculate high-frequency radiation from earthquake sources having spatially variable rupture velocity and stress drop, *Bull. Seismol. Soc. Am.*, *74*, 2061-2082, 1984.

Wald, D. J., and T. H. Heaton, Spatial and temporal distribution of slip for the 1992 Landers, California, earthquake, *Bull. Seismol. Soc. Am.*, *84*, 668-691, 1994.

Wald, D. J., D. V. Helmberger, and T. H. Heaton, Rupture model of the 1989 Loma Prieta earthquake from the inversion of strong-motion and broadband teleseismic data, *Bull. Seismol. Soc. Am.*, *81*, 1540-1572, 1991.

Wallace, R. E., Eyewitness account of surface faulting during the earthquake of 28 October 1983, Borah Peak Idaho, *Bull. Seismol. Soc. Am.*, *74*, 1091-1094, 1984.

Weeks, J. D., Constitutive laws for high velocity frictional sliding and their influence on stress drop during unstable slip, *J. Geophys. Res.*, *98*, 17,637-17,648, 1993.

Yomogida, K., and T. Nakata, Large slip velocity of the surface rupture associated with the 1990 Luzon earthquake, *Geophys. Res. Lett.*, *21*, 1799-1802, 1993.

G. C. Beroza, Department of Geophysics, Stanford University, Stanford, CA, 94305-2215. (e-mail: beroza@pangea.stanford.edu)

T. Mikumo, Instituto de Geofisica, Universidad Nacional Autonoma de Mexico, Ciudad Universitaria, Mexico 04510 D. F.

(Received February 20, 1996; revised July 9, 1996; accepted July 18, 1996.)